

## THE PRESSURE OF THE STAR FORMING ISM IN COSMOLOGICAL SIMULATIONS

FERAH MUNSHI<sup>1,6</sup>, CHARLOTTE CHRISTENSEN<sup>3</sup>, THOMAS R. QUINN<sup>1</sup>, FABIO GOVERNATO<sup>1</sup>, JAMES WADSLEY<sup>2</sup>, SARAH LOEBMAN<sup>4</sup>, SIJING SHEN<sup>5</sup>

*Draft version August 25, 2018*

### ABSTRACT

We examine the pressure of the star-forming interstellar medium (ISM) of Milky-Way sized disk galaxies using fully cosmological SPH+N-body, high resolution simulations. These simulations include explicit treatment of metal-line cooling in addition to dust and self-shielding, H<sub>2</sub> based star formation. The 4 simulated halos have masses ranging from a few times 10<sup>10</sup> to nearly 10<sup>12</sup> solar masses. Using a kinematic decomposition of these galaxies into present-day bulge and disk components, we find that the typical pressure of the star-forming ISM in the present-day bulge is higher than that in the present-day disk by an order of magnitude. We also find that pressure of the star-forming ISM at high redshift is on average, higher than ISM pressures at low redshift. This explains the why the bulge forms at higher pressures: the disk assembles at lower redshift, when the ISM is lower pressure and the bulge forms at high redshift, when the ISM is at higher pressure. If ISM pressure and IMF variation are tied together as suggested in studies like Conroy & van Dokkum (2012), these results could indicate a time-dependent IMF in Milky-Way like systems, as well as a different IMF in the bulge and the disk.

*Subject headings:* galaxies : star formation — galaxies : evolution — methods : numerical — N-body simulations

### 1. INTRODUCTION

The origin of the stellar initial mass function (IMF) is paramount to our understanding of star formation, stellar evolution and feedback and galaxy formation. The IMF influences most of the observable properties of both stellar populations and galaxies. Detecting variations of the IMF will provide deep insights into the process by which stars form including but not limited to: the origin of the stellar mass scale, the effects of metallicity and environment and the energetics of feedback. Additionally, the IMF is a key ingredient into a huge range of models of all the above phenomena, and a necessary assumption when deriving physical parameters from observations. Despite being such a vital ingredient, the origin and variations of the IMF still remain poorly understood.

In particular, of critical importance, is the question of whether the IMF is universal or whether the IMF is sensitive to the initial conditions of star formation—i.e., the structure of the ISM in which the stars are forming (see e.g. Kroupa et al. 2011). Growing observational evidence suggests that the high mass behavior of the IMF is uniform, including observations of the IMF in the Magellanic Clouds (Kroupa & Weidner 2003; Bastian et al. 2010; Chabrier 2003). However at the low mass end, there are many indications, both obser-

vationally and theoretically, that there may be a variation in the IMF. For example, Conroy & van Dokkum (2012) and van Dokkum & Conroy (2011) show that the IMF in these systems is bottom heavy using gravity sensitive absorption lines in the cores of giant elliptical galaxies. This has also been independently suggested by kinematic and lensing data (Treu et al. 2010; Cappellari 2012; Dutton et al. 2013). As these systems formed their stars at high redshift, these studies give us insight into the time-evolution of the IMF. Observationally, Conroy & van Dokkum (2012) show that the mass to light ratios of spheroidal systems indicate a more bottom heavy IMF at higher pressures, and at higher SFRs. This indicates that ISM pressure and the intensity of star formation are both key in understanding how and where stars form- and whether or not the IMF is varying.

Despite the importance of the IMF, a universally agreed upon, fully cosmological, physical theory of its origin and variation with environment has yet to be found: rather, many competing models exist. In particular, explaining the evolution of the IMF has been a challenge for theoretical models, especially in 'normal' systems. In general, these studies predict large IMF variations with local thermal Jeans Mass (Larson 1998, 2005), Mach number of the star-forming ISM, or the distribution of densities in a supersonically turbulent ISM (Padoan et al. 1997, 2012; Hennebelle & Chabrier 2008; Hopkins 2012b,a). Most theoretical models offer explanations of IMF variation in more extreme conditions—ULIRG, nuclear starbursts owing to the extreme mergers and large gas inflows (Kormendy & Sanders 1992; Hopkins et al. 2008; Hopkins 2013; Narayanan & Davé 2012; Narayanan & Hopkins 2013) but many predict a top-heavy scenario, contradictory to the observational evidence. Furthermore, Krumholz (2011) shows that the critical mass, i.e. the fragmentation mass of a col-

<sup>1</sup> Department of Astronomy, University of Washington, Seattle, WA

<sup>2</sup> Department of Physics and Astronomy, McMaster University, Hamilton, ON, Canada

<sup>3</sup> Department of Astronomy, University of Arizona, 933 North Cherry Ave, Rm. N204, Tucson AZ 85721

<sup>4</sup> Department of Astronomy, University of Michigan, 500 Church St Ann Arbor, Michigan 48109

<sup>5</sup> Department of Astronomy, University of California, Santa Cruz, 1156 High Street, ISB Bldg Room 211, Santa Cruz, CA 95064

<sup>6</sup> email address: fdm@astro.washington.edu

lapping star-forming cloud, is dependent on the metallicity and pressure of the cloud itself. In a toy model, Weidner et al. (2013) suggest a time dependent IMF with a top heavy IMF slope followed by a prolonged bottom heavy slope which will bring the ISM pressure, temperature and turbulence into states that will drastically alter fragmentation of the gas, to explain observations.

In this letter, we perform SPH+ $N$ -body simulations of four medium-mass galaxies to directly explore the star-forming ISM in a cosmological context. This study is unique in that SPH simulations, being particle based, allow us to follow the full thermodynamic history of the gas. Furthermore, the resolution and star formation recipe in these simulations allow us to begin to probe the density structure of a more realistic star-forming ISM, in a cosmological setting. Here we specifically focus on a comparison between the star forming ISM of stars that make up the *present-day* bulge and those that make up the *present-day* disk. We find that stars form at ISM pressures an order of magnitude higher in the bulge than those in the disk, on average. Additionally, we find that at early times both bulge and disk stars form in a high pressure ISM. Finally, we find that differences in the formation radius of bulge and disk stars are not responsible for the different pressures. In short, we show that there ISM pressure varies with time, which could imply that the IMF varies with time as well.

## 2. SIMULATIONS AND ANALYSIS

The simulations used in this work were run with the N-Body + SPH code GASOLINE (Wadsley et al. 2004; Stinson et al. 2006) in a fully cosmological  $\Lambda$ CDM context:  $\Omega_0 = 0.26$ ,  $\Lambda = 0.74$ ,  $h = 0.73$ ,  $\sigma_8 = 0.77$ ,  $n = 0.96$ . Using the ‘zoomed-in’ volume renormalization technique (Katz & White 1993; Pontzen et al. 2008), we selected from uniform DM-only simulations field-like regions which we then resimulated at higher resolution. This set of simulations includes metal line cooling (Shen et al. 2010) and tracks non-equilibrium  $H_2$  abundances (Christensen et al. 2012b, hereafter CH12). As in CH12, the star formation rate (SFR) in our simulations is set by the local gas density and the  $H_2$  fraction;  $SF \propto (f_{H_2} c_* \times \rho_{gas})^{1.5}$ , with  $c_* = 0.1$ . Star formation is limited to gas with density greater than 0.1 amu/cc and temperature less than 3000 K, although the dependency of star formation on the  $H_2$  abundance makes these limitations largely inconsequential. Tests of the convergence of star formation histories for this star formation prescription are described in CH12.

The full details of our SN feedback ‘blastwave’ approach are described in several papers including, Stinson et al. (2006); Governato et al. (2012). As massive stars evolve into SN, mass, thermal energy and metals are deposited into nearby gas particles, with energy of  $10^{51}$  ergs per event. Gas cooling is shut-off until the end of the snow-plov phase as described the Sedov-Taylor solution, typically ten million years. We also include gas heating from a uniform, time evolving UV cosmic background, which turns on at  $z = 9$  and modifies the ionization and excitation state of the gas, following the model of Haardt & Madau (1996). The efficient deposition of SN energy into the ISM, and the modeling of recurring SN by the Sedov solution, should be interpreted as a proxy we have tuned to model the effect of pro-

Galaxy Name	$M_{halo}$ ( $M_\odot$ )	Gas Mass ( $M_\odot$ )	Particle	Softening (pc)
h986	$1.9 \times 10^{11}$	3900		115
h277	$6.8 \times 10^{11}$	3900		115
h258	$7.7 \times 10^{11}$	3900		115
h239	$9.1 \times 10^{11}$	3900		115

TABLE 1  
DESCRIPTION OF SIMULATIONS UTILIZED IN THIS ANALYSIS.

cesses related to young stars and to model the effect of energy deposited in the local ISM including UV radiation from massive stars (Hopkins et al. 2011; Wise et al. 2012). The simulations also include a scheme for turbulent mixing that redistributes heavy elements among gas particles (Shen et al. 2010). These feedback, star formation, and ISM parameters in simulations of the same resolution produced galaxies with realistically-concentrated bulges (Christensen et al. 2012a). Furthermore, it is important to note that because the simulations are tuned to produce realistic present-day galaxies (see e.g. Munshi et al. (2013)), with correct surface densities, the mean ISM pressure in these simulations should be approximately correct, even if the feedback model does not include processes specifically related to young stars, stellar winds and radiation pressure (Hopkins et al. 2011; Hopkins 2013).

We have simulated four different disk galaxies, at high resolution, described in Table 1. We dynamically decompose our disk galaxies based on cuts in angular momentum and energy (Scannapieco et al. 2011; Governato et al. 2009). Each star particle at  $z = 0$  is traced back to the gas particle from which it formed in order in order to sample the properties of the ISM from which each component formed. Using the cold gas in the central few kiloparsecs of the galaxy, a star particle is established as disk when its specific angular momentum ( $j_z$ ) is a large fraction of the angular momentum of a circular orbit with the same binding energy, i.e.,  $j_z/j_c > 0.8$ . Using the potential of the entire matter distribution (dark, gas and stars), we determine the total energy for each particle and subsequently its angular momentum. For the bulge and halo stars, star particles are identified based on their radial orbits and their binding energy: bulge stars have higher binding energies than halo stars. Furthermore bulge and halo are also distinguished by the radius where the spheroid mass profile changes to a shallower slope. We checked the stability of our kinematic decomposition across three simulation outputs in time- ie over the course of 100 Myr which approximates the dynamical time of the systems. We compared the results of our analysis in the case of the strictest definition that particles must be classified as the same component over a whole dynamical time to the weakest definition that particles need only be classified a component at  $z = 0$  and found that the resulting trends remain unchanged.

Using full information from the simulations (kinematics, ages, metallicity), we have traced the density, temperature, velocity dispersion and pressure of the ISM in which the stars of each component form. Being particle based, the SPH approach of our simulations allows us to follow in detail the thermodynamical history of the gas through cosmic times, without resorting to additional

‘tracer elements’ (Genel et al. 2013). This allows us to examine not only where, but also *in what environment* stars are forming in our simulated Milky-Way like galaxies. In our analysis, we define pressure in very simple terms:  $P = nk_bT$ . We get temperature and density by tracing each star particle belonging to disk and bulge back to the gas particle from which it formed. Each gas particle is tagged with a local density and temperature that is a function of the simulation force resolution and softening length. Gas properties are calculated based on the 32 nearest neighbors. Our definition of pressure is limited to a “thermal” pressure term, which, as we do not resolve disks of highly turbulent gas, is actually a proxy for the entire pressure in the gas. Namely, it is the primary pressure support against the gravitational pressure in the disk.

### 3. RESULTS

In this section we show that ISM structure is closely tied to star formation. Additionally, we show that at earlier times in a galaxy’s history, stars are forming in a higher pressure ISM environment than that in which stars form today. This is theoretical evidence for a variation in IMF in a “normal” Milky-Way environment, if IMF variations are indeed tied to ISM structural parameters, like temperature, density, metallicity and pressure (Conroy & van Dokkum 2012; Krumholz 2011). For brevity, we show plots for one of our simulated halos, demonstrating the trends observed for all four halos.

In all four simulated halos, each cosmological and with varying merger and star formation histories, the distribution of pressure values in the ISM that forms *the present day* bulge is higher by an order of magnitude than that which forms the *present day* disk. In Figure 1a, we show the distribution of formation pressures for one of our simulated Milky-Ways, h986. The peak pressure of both distributions is different: bulge stars peak at pressures an order of magnitude higher pressure than disk stars. This shows that in general, bulge stars are forming ISM that is structurally different in terms of gas temperature and density: specifically, stars are forming from denser gas. It is important to note that the actual values for pressure are not comparable to pressures found in observations. As our star formation prescription is resolution limited, the maximum gas densities achieved are resolution dependent. What should be highlighted is the *relative* difference between the pressures found in the bulge and disk of our simulated galaxies. In Figure 1b and 1c, we show the SFHs for the 3 simulated halos, not directly discussed here, to show that in general, for all halos, the bulge forms at early times, and the disk forms later.

In Figure 2 we compare the phase diagrams for bulge and disk during a star formation event which contributes to the components’ overall mass growth: for the bulge, this was between 2.5 and 4 Gyrs and for the disk, between 10 and 13 Gyrs. This figure at first glance, demonstrates that in general, the bulge forms in a range of densities that is higher than that of the disk, and that the temperature range is very similar. Each point in the phase diagrams is color coded according to pressure where hotter colors represent higher pressures (red is the highest pressure bin). This color-coding further drives home that it is the high densities in the bulge star formation event that drive the high pressures, while in the disk, the high

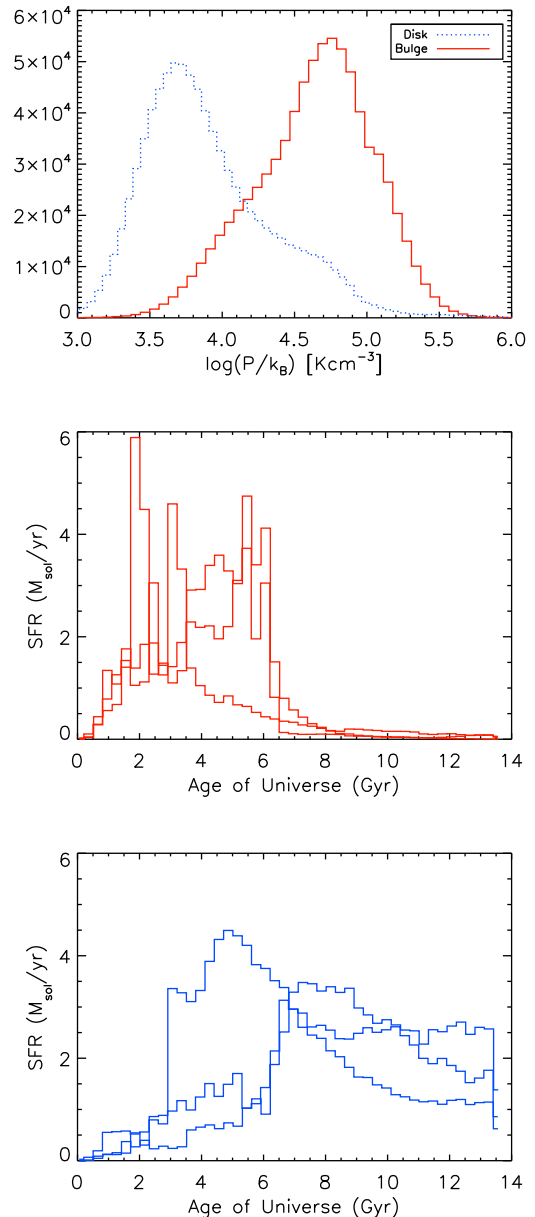


FIG. 1.— *Top Panel:* Distribution of pressures for bulge and disk in one of the simulated galaxies, h986. Note that the peak of the distribution of pressures of the bulge is higher than the peak of the pressure distribution of disk stars. *Middle Panel:* SFHs for the bulges of the 3 galaxies not shown in this manuscript. Note that like h986 shown in Figure 3, the bulges form early in the galaxy’s history. *Bottom Panel:* SFHs for the disks of the 3 galaxies not shown in this manuscript. As with the bulges, these galaxies also follow the same trend as h986, with disk star formation occurring later in the galaxy’s history.

pressures result from higher temperatures. Since our simulations use an  $H_2$ -dependent star formation recipe, low metallicity gas particles would be expected to form stars at higher densities. However, from the bottom panel of Figure 2 it is clear that even at the same metallicities, bulge stars form from denser gas.

In Figure 3, we present the star formation history for the same galaxy, h986, for the dynamical bulge (red) and disk (blue). We also present the median pressure as

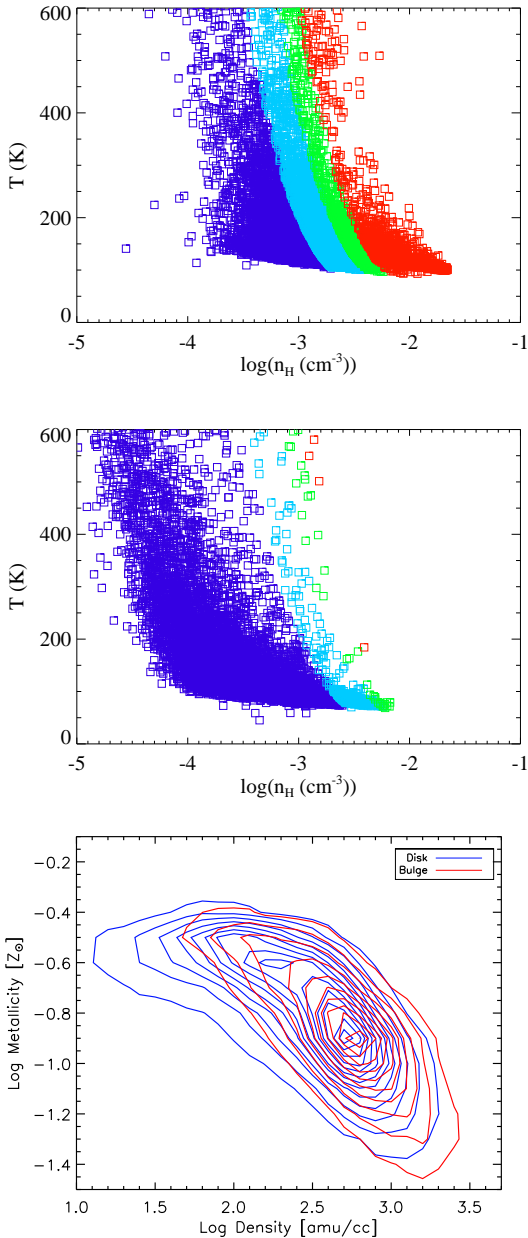


FIG. 2.— Phase Diagrams for bulge (top) and disk (bottom) during a star formation event, color coded by pressure. Star formation events for each component were selected based on contribution to each components’ overall growth. Hotter colors are higher pressures, cooler colors are lower pressures. Note that high pressures are driven by high densities in the bulge. In the bottom panel we show the metallicity of the gas that formed both the bulge and disk stars versus its density at the time of star formation (note that both density and metallicity are smoothed over hundreds of parsecs).

a function of time for both components in the same time bins. Figure 2 highlights that both components are forming stars at higher pressures early in the galaxy’s history. The star formation histories show that the bulge forms the majority of its stars early on, when typical ISM pressures are high, while the disk forms its stars later, when ISM pressures are lower. We also can see the parallel in the bulge SFH and the bulge pressure, in that bursts of

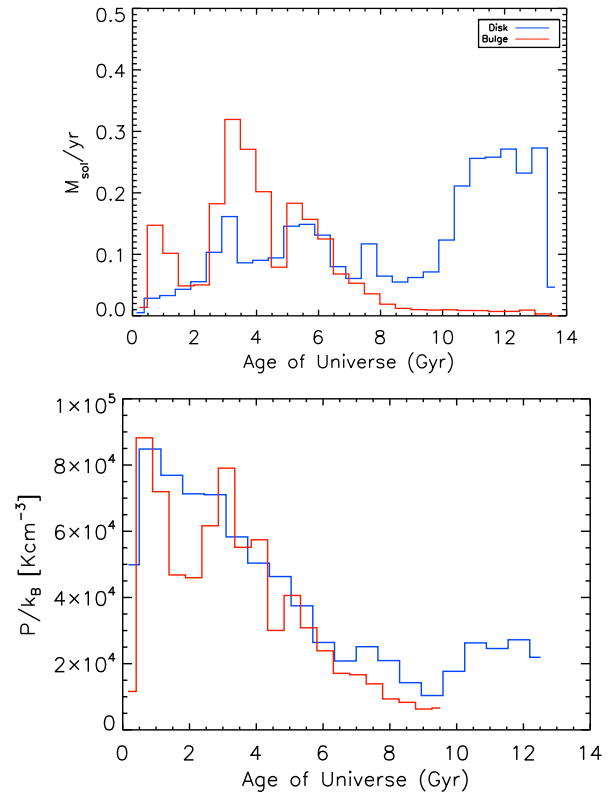


FIG. 3.— Top Panel: Star formation rates for each of the dynamical components of *h986*. Bottom Panel: Pressure vs. Time for each of the components. This highlights the redshift dependence of the pressure of the star forming ISM: early on, stars are forming at higher pressures, regardless of which component they belong to at  $z = 0$ . Note also the peaks in pressure are present when the SFH is peaking, in bulge stars. The big bursts in the bulge SFH correspond to major mergers in the galaxy’s history.

bulge star formation seem to be contemporaneous with ISM pressure peaks. We discuss what this may imply in the summary.

Finally, in Figure 4, we explore whether formation location has any bearing on the pressure of the gas. We expect that pressure is higher closer to the center of the galaxy (i.e., where one would expect to find bulge stars), given that the vertical gravity and surface density should be higher closer to the center. As a result, one would expect high pressures towards the center of the galaxy. However, Figure 3 shows that this explanation cannot entirely explain the pressure differential between bulge and disk. In the top panel we see that there is no correlation between formation radius and pressure for either component, over the galaxy’s whole history and that bulge stars are in forming at higher pressures than disk stars. In the second panel, we look only at the stars that formed in the early protogalaxy: specifically, the gas that forms stars that are 6 Gyrs old or more, when both components are should be at higher pressures. We see that with that cut, at any formation radius, bulge stars and disk stars are forming at high pressures in the early universe, implying the existence of an early high pressure star-forming environment in the protogalaxy.

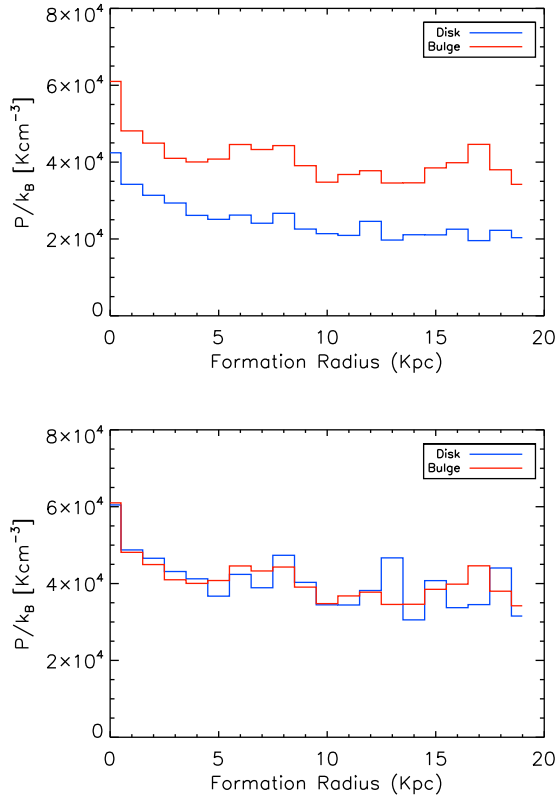


FIG. 4.— Top Panel: Pressure vs. formation radius for the bulge and disk, over the galaxy’s whole history. Bottom Panel: Pressure vs. formation radius for each of the components, for stars that formed before 6 Gyrs (when the pressure of the ISM was higher for both components). This figure highlights that formation radius is not the underlying cause of the pressure differential between bulge and disk and that on average, bulge stars are forming at higher pressures than disk stars. The bottom panel shows that in the first half of the galaxy’s history, stars are forming at higher pressures in general, regardless of component and formation radius.

In this letter, we provide evidence that ISM pressure is redshift dependent by examining the ISM pressures during the formation of the present-day bulge and disk. Because the present-day bulge predominantly forms early in the galaxy’s history, it forms at higher pressures than

the present-day disk. We show that in general, at early times, star formation occurs at higher pressures—specifically higher densities. We show that this is not the result of formation location and the higher densities found in the center of the protogalaxy: in general bulge and disk stars are forming over all formation radii. If ISM pressure and IMF are related as postulated in Krumholz (2011); Conroy & van Dokkum (2012), we have evidence for a redshift dependence of the IMF and further, that bulge stars formed with a different IMF from disk stars. Furthermore, we show that even at high redshift, bulge stars and disk stars in general, are forming at higher pressures, regardless of formation radius. This further supports the redshift dependence of ISM pressure: we see that in the young protogalaxy stars form in a high pressure disk, regardless of classification at  $z = 0$ . However, as Figure 3 demonstrates, the majority of bulge stars are formed in this high-pressure star formation epoch, while the majority of disk stars form in the later, low-pressure epoch. In our analysis we also examine the differences in metallicity and  $\text{H}_2$  fraction between bulge and disk, to isolate why the early protogalaxy is at high density (and thus high pressure). We find that bulge stars form from gas with higher  $\text{H}_2$  fractions and even when holding metallicity constant, bulge stars form from denser gas. These trends point toward the high redshift progenitors having more dense gas, likely as a result of early rapid accretion.

Future work will include following the assembly history of these galaxies to determine the role of mergers and gas accretion in the formation of the present-day bulge and disk. We will follow the build-up of each component tracing each star back in time, including a full merger tree. In this way we can determine isolate the role of mergers and in-situ star formation on the structure of the star-forming ISM

FDM, CC, TQ and FG gratefully acknowledge the support by NSF award AST-0908499. FDM also gratefully acknowledges support from the Washington Space Grant Fellowship. Simulations were run using computer resources and technical support from NAS. The authors thank Alyson Brooks, Jillian Bellovary, and Michael Tremmel for assistance and helpful comments, as well as the anonymous referee who greatly improved this manuscript.

#### REFERENCES

- Bastian, N., Covey, K. R., & Meyer, M. R. 2010, *ARA&A*, 48, 339  
 Cappellari, M. 2012, ArXiv e-prints  
 Chabrier, G. 2003, *PASP*, 115, 763  
 Christensen, C., Governato, F., Quinn, T., Brooks, A. M., Fisher, D. B., Shen, S., McCleary, J., & Wadsley, J. 2012a, ArXiv e-prints  
 Christensen, C., Quinn, T., Governato, F., Stilp, A., Shen, S., & Wadsley, J. 2012b, *MNRAS*, 425, 3058  
 Conroy, C., & van Dokkum, P. G. 2012, *ApJ*, 760, 71  
 Dutton, A. A., Macciò, A. V., Mendel, J. T., & Simard, L. 2013, *MNRAS*, 432, 2496  
 Genel, S., Vogelsberger, M., Nelson, D., Sijacki, D., Springel, V., & Hernquist, L. 2013, *MNRAS*  
 Governato, F. et al. 2009, *MNRAS*, 398, 312  
 —. 2012, ArXiv e-prints  
 Haardt, F., & Madau, P. 1996, *ApJ*, 461, 20  
 Hennebelle, P., & Chabrier, G. 2008, *ApJ*, 684, 395  
 Hopkins, A. M., McClure-Griffiths, N. M., & Gaensler, B. M. 2008, *ApJ*, 682, L13  
 Hopkins, P. F. 2012a, *MNRAS*, 423, 2016  
 —. 2012b, *MNRAS*, 423, 2037  
 —. 2013, *MNRAS*, 428, 2840  
 Hopkins, P. F., Quataert, E., & Murray, N. 2011, ArXiv e-prints  
 Katz, N., & White, S. D. M. 1993, *ApJ*, 412, 455  
 Kormendy, J., & Sanders, D. B. 1992, *ApJ*, 390, L53  
 Kroupa, P., & Weidner, C. 2003, *ApJ*, 598, 1076  
 Krumholz, M. R. 2011, *ApJ*, 743, 110  
 Larson, R. B. 1998, *MNRAS*, 301, 569  
 Larson, R. B. 2005, in *Astrophysics and Space Science Library*, Vol. 327, The Initial Mass Function 50 Years Later, ed. E. Corbelli, F. Palla, & H. Zinnecker, 329  
 Munshi, F. et al. 2013, *ApJ*, 766, 56  
 Narayanan, D., & Davé, R. 2012, *MNRAS*, 423, 3601  
 Narayanan, D., & Hopkins, P. F. 2013, *MNRAS*, 433, 1223  
 Padoan, P., Haugbølle, T., & Nordlund, Å. 2012, *ApJ*, 759, L27  
 Padoan, P., Nordlund, A., & Jones, B. J. T. 1997, *MNRAS*, 288, 145  
 Pontzen, A. et al. 2008, *MNRAS*, 390, 1349

- Scannapieco, C., White, S. D. M., Springel, V., & Tissera, P. B. 2011, *MNRAS*, 417, 154
- Shen, S., Wadsley, J., & Stinson, G. 2010, *MNRAS*, 407, 1581
- Stinson, G., Seth, A., Katz, N., Wadsley, J., Governato, F., & Quinn, T. 2006, *MNRAS*, 373, 1074
- Treu, T., Auger, M. W., Koopmans, L. V. E., Gavazzi, R., Marshall, P. J., & Bolton, A. S. 2010, *ApJ*, 709, 1195
- van Dokkum, P. G., & Conroy, C. 2011, *ApJ*, 735, L13
- Wadsley, J. W., Stadel, J., & Quinn, T. 2004, *New Astronomy*, 9, 137
- Weidner, C., Ferreras, I., Vazdekis, A., & La Barbera, F. 2013, *MNRAS*
- Wise, J. H., Turk, M. J., Norman, M. L., & Abel, T. 2012, *ApJ*, 745, 50

## REFERENCES

- Bastian, N., Covey, K. R., & Meyer, M. R. 2010, *ARA&A*, 48, 339
- Cappellari, M. 2012, *ArXiv e-prints*
- Chabrier, G. 2003, *PASP*, 115, 763
- Christensen, C., Governato, F., Quinn, T., Brooks, A. M., Fisher, D. B., Shen, S., McCleary, J., & Wadsley, J. 2012a, *ArXiv e-prints*
- Christensen, C., Quinn, T., Governato, F., Stilp, A., Shen, S., & Wadsley, J. 2012b, *MNRAS*, 425, 3058
- Conroy, C., & van Dokkum, P. G. 2012, *ApJ*, 760, 71
- Dutton, A. A., Macciò, A. V., Mendel, J. T., & Simard, L. 2013, *MNRAS*, 432, 2496
- Genel, S., Vogelsberger, M., Nelson, D., Sijacki, D., Springel, V., & Hernquist, L. 2013, *MNRAS*
- Governato, F. et al. 2009, *MNRAS*, 398, 312
- . 2012, *ArXiv e-prints*
- Haardt, F., & Madau, P. 1996, *ApJ*, 461, 20
- Hennebelle, P., & Chabrier, G. 2008, *ApJ*, 684, 395
- Hopkins, A. M., McClure-Griffiths, N. M., & Gaensler, B. M. 2008, *ApJ*, 682, L13
- Hopkins, P. F. 2012a, *MNRAS*, 423, 2016
- . 2012b, *MNRAS*, 423, 2037
- . 2013, *MNRAS*, 428, 2840
- Hopkins, P. F., Quataert, E., & Murray, N. 2011, *ArXiv e-prints*
- Katz, N., & White, S. D. M. 1993, *ApJ*, 412, 455
- Kormendy, J., & Sanders, D. B. 1992, *ApJ*, 390, L53
- Kroupa, P., & Weidner, C. 2003, *ApJ*, 598, 1076
- Krumholz, M. R. 2011, *ApJ*, 743, 110
- Larson, R. B. 1998, *MNRAS*, 301, 569
- Larson, R. B. 2005, in *Astrophysics and Space Science Library*, Vol. 327, *The Initial Mass Function 50 Years Later*, ed. E. Corbelli, F. Palla, & H. Zinnecker, 329
- Munshi, F. et al. 2013, *ApJ*, 766, 56
- Narayanan, D., & Davé, R. 2012, *MNRAS*, 423, 3601
- Narayanan, D., & Hopkins, P. F. 2013, *MNRAS*, 433, 1223
- Padoan, P., Haugbølle, T., & Nordlund, Å. 2012, *ApJ*, 759, L27
- Padoan, P., Nordlund, A., & Jones, B. J. T. 1997, *MNRAS*, 288, 145
- Pontzen, A. et al. 2008, *MNRAS*, 390, 1349
- Scannapieco, C., White, S. D. M., Springel, V., & Tissera, P. B. 2011, *MNRAS*, 417, 154
- Shen, S., Wadsley, J., & Stinson, G. 2010, *MNRAS*, 407, 1581
- Stinson, G., Seth, A., Katz, N., Wadsley, J., Governato, F., & Quinn, T. 2006, *MNRAS*, 373, 1074
- Treu, T., Auger, M. W., Koopmans, L. V. E., Gavazzi, R., Marshall, P. J., & Bolton, A. S. 2010, *ApJ*, 709, 1195
- van Dokkum, P. G., & Conroy, C. 2011, *ApJ*, 735, L13
- Wadsley, J. W., Stadel, J., & Quinn, T. 2004, *New Astronomy*, 9, 137
- Weidner, C., Ferreras, I., Vazdekis, A., & La Barbera, F. 2013, *MNRAS*
- Wise, J. H., Turk, M. J., Norman, M. L., & Abel, T. 2012, *ApJ*, 745, 50